RSC Advances

This is an *Accepted Manuscript*, which has been through the Royal Society of Chemistry peer review process and has been accepted for publication.

Accepted Manuscripts are published online shortly after acceptance, before technical editing, formatting and proof reading. Using this free service, authors can make their results available to the community, in citable form, before we publish the edited article. This *Accepted Manuscript* will be replaced by the edited, formatted and paginated article as soon as this is available.

You can find more information about *Accepted Manuscripts* in the Information for Authors.

Please note that technical editing may introduce minor changes to the text and/or graphics, which may alter content. The journal's standard Terms & Conditions and the Ethical guidelines still apply. In no event shall the Royal Society of Chemistry be held responsible for any errors or omissions in this *Accepted Manuscript* or any consequences arising from the use of any information it contains.

ROYAL SOCIETY OF CHEMISTRY

www.rsc.org/advances

1 **Fabrication of resistive switching gallium oxide thin film with tailoring gallium
2 valence state and oxygen deficiency by rf cosputtering process**

3

4 Chiharu Kura[1], Yoshitaka Aoki[2*] Etsushi Tsuji[2], Hiroki Habazaki[2] and Manfred Martin[3]

5

6 [1]Graduate School of Chemical Science & Engineering, Hokkaido University, N13W8
7 Kita-ku, Sapporo, 060-8628 Japan.
8 [2]Faculty of Engineering, Hokkaido University, N13W8 Kita-ku, Sapporo, 060-8628
9 Japan.
10 [3]Institute of Physical Chemistry, RWTH Aachen University and JARA-FIT, 52056
11 Aachen, Germany.

12

13 E-mail address for correspondence : y-aoki@eng.hokudai.ac.jp

14

15

RSC Advances Accepted Manuscript

1 **Abstract**

2 Resistive switching gallium oxide base thin films with tailoring oxygen deficiency were
3 fabricated by rf cosputtering of Ga_2O_3 and Cr. XPS and STEM-EDX analysis disclosed
4 that the resultant film was made of homogeneous oxide glass layer with mixed valance
5 states of Ga(III)-Ga(I). The amount of Ga(I) and the corresponding oxygen deficiency
6 were precisely controlled because the following redox reaction subsequently progresses
7 in the deposited films: 3Ga(III) + 2Cr(0) → 3Ga(I) + 2Cr(III). The on/off resistance
8 ratio was largely varied by changing Ga(I) fraction in relation to the oxide ion
9 conductivity, and $Ga_{0.82}Cr_{0.18}O_{1.2}$ thin film was found to exhibit optimal switching
10 performance. The film resistance state was tunable by a 100's μs pulse biasing and was
11 incrementally changed by increasing applied pulse numbers. The strongly
12 time-dependent switching events and area dependent current level of Cr-GaO_x films was
13 distinct from the abrupt switching behavior of filamentary mechanism TiO_x thin film
14 devices. It was demonstrated that rf cosputtering of the metal oxides and the
15 corresponding oxygen scavenging metals was a powerful technique to design the bulk
16 state resistive switching devices based on nonstoichiometric metal oxide thin film.

17

18 **Key words**: resistive switching, gallium oxide, gallium suboxide, rf sputtering

19

RSC Advances Accepted Manuscript

1 **Introduction**

2 As the potential next generation for nonvolatile memory, resistive random access
3 memory (RRAM) with a simple metal/oxide/metal sandwich structure has been studied
4 intensively during the past decades.[1] In case of the well-established Pt/TiO_2/Pt
5 memristor devices, the switching between high resistance state (HRS) and low
6 resistance state (LRS) is triggered by the modification of the tunnel barrier width
7 between a top electrode (TE) and the preformed conductive filament due to the ionic
8 drift within a few nanometre-thick space charge layer in vicinity of the interface with
9 electrode.[2-4]

10 Gallium oxide devices are considered as one of ideal candidates for RRAM because
11 of its intrinsic high resistance characteristic and extraordinarily sensitive conductivity to
12 the oxygen concentration.[5-9] In a previous study, we found resistive switching in
13 highly-nonstoichiometric, amorphous gallium oxide thin films, *a*-$GaO_{1.1}$ was originated
14 from the bulk mixed oxide ion-electron conductivity.[8] The homogeneous migration of
15 oxygen vacancy donors modify the electronic carrier distribution across films and thus
16 resistance states of film bulk varies by applied fields.[8] Such a bulk-conduction
17 mechanism memristor could realize multilevel states of resistance and a large on/off
18 current ratio due to the continuous tunability of the internal state variable, and therefore
19 is expected to be a dynamical memristor system to emulate synaptic memory
20 behaviour.[10,11] To develop feasible homogeneous resistive switching devices for future

RSC Advances Accepted Manuscript

1 neuromorphic application, it is benefical to design amorphous gallium oxides with
2 enhanced ion conductivity. The oxide ion conductivity of *a*-GaO_x must be related with
3 interstitial spaces and local Ga environments of the mixed valence state Ga(III)-Ga(I)
4 oxide glasses. Therefore, it is of fundamental and of technological importance to
5 develop the precise fabrication process with tailoring the oxygen deficiency, namely,
6 Ga(I) fractions in the oxide matrices in order to tune the resistive switching properties
7 of film devices.

8 Highly-nonstoichiometric amorphous GaO_x thin films have been fabricated by pulse
9 laser deposition (PLD) with a Ga_2O_3 target under low p_{O2} conditions.[5,8,9] Unfortunately,
10 it is difficult to control the yields of Ga(I) suboxides by the method because Ga_2O_3 is
11 not easily reduced under extremely low O_2 pressure at elevated temperature.[12] Lee et al
12 reported the fabrication of oxygen deficient gallium oxide films by high temperature
13 vacuum annealing of Ga_2O_3/Cr/Ga_2O_3 three layer laminates.[6] Gallium oxide is
14 efficiently reduced through the interdiffusion reaction because of relatively large
15 negative energy of Cr-O bonding (-1053 kJ mol^{-1}) in comparison to Ga-O bonding
16 (-998.3 kJ mol^{-1}).[13] Such a redox reaction must be useful to prepare the Ga(I)-Ga(III)
17 mixed valence gallium oxide. Herein, we successfully fabricated Cr-doped gallium
18 oxide films with a controlled amount of Ga(I) and oxygen deficiency by depositing a
19 homogeneous mixture of Ga(III) oxide moieties and Cr(0) metal atoms. The chromium
20 atoms scavenge the oxygen atoms of Ga(III) oxide moieties and thus Ga(I)-Ga(III)

RSC Advances Accepted Manuscript

1 mixed valence state homogeneous oxide glass was prepared. The films with optimal
2 amount of Ga(I) fractions revealed remarkable bulk resistive switching with large on/off
3 ratio according to the efficient oxide ion conductivity, which enables incremental
4 change of the bulk resistance state by increasing bias duration or applied short pulse
5 numbers. The switching behavior was compared to the well-established TiO_x thin film
6 base filamentary mechanism switching devices.

7

8 **Experimental**

9 A 20 nm-thick Pt deposited Si wafer (100) was used as a bottom electrode (BE).
10 Nonstoichiometric TiO_x and Cr-doped GaO_x thin films were deposited on a Pt BE by rf
11 sputtering at room temperature. TiO_x thin films were deposited by using a Ti target
12 (purity: 99.9%) in a mixed argon and oxygen atmosphere (the ratio of Ar/O_2 was 5:1) at
13 a total pressure of 0.4 Pa at substrate temperature of 150°C. Cr-doped GaO_x films
14 (Cr-GaO_x) were deposited by cosputtering with Ga_2O_3 and Cr targets in pure argon
15 atmosphere at a pressure of 1 Pa. The sputtering power of Ga_2O_3 was fixed at 50 W and
16 that of Cr was adjusted at 30, 40, 60 and 70 W in order to change Ga/Cr molar ration in
17 the resultant film. The substrate was kept at ambient temperature. Circular metal top
18 electrodes (TE) with a diameter of 100-800 μm and a thickness of 50 nm were
19 sputter-deposited on the films through a metal shadow mask. The *I-V* characteristics of
20 the devices were measured at room temperature using a source-measure units

RSC Advances Accepted Manuscript

1 (KEITHLEY 2601B). In all cases, Pt TE is firstly swept from 0 V to anodic region (+ 1
2 V), swept back to cathodic region (- 1 V) and returned to 0 V so as to complete one
3 cycle of voltage sweep. The voltage steps are fixed at 0.1 V.

4 The chemical composition of Cr-GaO_x films was examined by wave-length dispersive
5 X-ray analysis (WDX) with a JEOL JXA-8530F. For WDX measurements, 800
6 nm-thick films were deposited on the Pt/Si wafer by sputtering under the same
7 atmospheric, rf power and temperature conditions as those for the corresponding
8 switching device films. The cross-sectional transmission electron microscopy (TEM)
9 and energy dispersive X-ray fluorescent analysis (EDX) were carried out in a HITACHI
10 HD-2000. The specimens for TEM observation were prepared by a focused ion beam
11 microfabrication (FIB; HITACHI FB-2100). X-ray photoelectron spectroscopy (XPS)
12 was carried out in JEOL JPS-9010MC with Mg Kα radiation. The depth profile was
13 applied by *in situ* Ar^+ ion sputtering. The curve fitting were carried out with
14 Lorenz-Gaussian function.

15

16 **Results**

17 Firstly, GaO_x films are fabricated by sputtering a single Ga_2O_3 target. The resulting
18 films are transparent, indicating amount of oxygen deficiency in the film is quite small.
19 On the other hand, the uniform, dark-colored thin film can be obtained by cosputtering
20 of Cr and Ga_2O_3. The chemical composition of the films deposited with a Cr sputtering

RSC Advances Accepted Manuscript

1 power of 30, 40, 60 and 70 W is $Ga_{0.96\pm0.02}Cr_{0.04\pm0.02}O_{1.4\pm0.1}$, $Ga_{0.91\pm0.04}Cr_{0.09\pm0.05}O_{1.3\pm0.1}$,
2 $Ga_{0.82\pm0.2}Cr_{0.18\pm0.02}O_{1.2\pm0.1}$ and $Ga_{0.78\pm0.06}Cr_{0.22\pm0.03}O_{1.2\pm0.1}$ respectively, as determined by
3 WDX measurements (Table 1). These films are hereafter called as Ga96Cr4, Ga91Cr9,
4 Ga82Cr18 and Ga78Cr22, respectively, based on the average metal composition. Figure
5 1(a) shows cross-sectional TEM of Ga82Cr18 thin films. The densely-packed films (120
6 nm thickness) are uniformly formed over a wide area of a Pt/Si wafer substrate.
7 Apparent pinholes and clacks are not observed. STEM-EDX shows chromium is
8 homogeneously distributed throughout the film bulk (Figs. 1(c) and (d)) without
9 segregation, indicating homogeneous mixtures of chromium and gallium oxide are
10 prepared by the cosputtering. The Ga82Cr18 thin films show only a halo ring, indicating
11 an amorphous phase (Fig. 1(b)).
12 Figure 2 shows Ga 3d and Cr 2p XPS spectra of 120 nm-thick Cr-GaO_x thin films.
13 In all cases, Ga 3d peak is deconvoluted into two peaks; a peak at 20.7 eV due to the
14 Ga(III) state and a peak at 19.6 eV due to Ga(I) state (Fig. 2a).[8,14] Ga(III)/Ga(I) molar
15 ratios in Ga96Cr4, Ga91Cr9, Ga82Cr18 and Ga78Cr22 are 90/10, 77/23, 69/31 and
16 64/36, respectively (Table 1). These values of the molar ratios are consistent with ones
17 calculated from chemical composition by accounting charge compensation between
18 cations (Ga^{3+}, Ga^{+} and Cr^{3+}) and anion (O^{2-}). On the other hand, Cr 2*p* XPS spectral
19 features are not changed by chemical composition (Fig. 2(b)). All films reveal apparent
20 spectral feature of Cr(III) with Cr $2p_{1/2}$ and $2p_{3/2}$ peaks at 587.5 eV and 577 eV,

RSC Advances Accepted Manuscript

1 respectively[15] while the features of lower valence state Cr, such as Cr(0) (574.2 eV of
2 $2p_{3/2}$)[16] and Cr(I) (576.3 eV of $2P_{3/2}$)[16] does not appear (Fig. 2(c)).
3 Ga 3d XPS spectra of Ga82Cr18 were also measured in the depth of about 50 nm
4 (middle) and 100 nm (near bottom edge) by Ar^+ ion milling (Fig. 2(c)). The spectra
5 show similar features at any depths (Fig. 2(b)), indicating Ga(I) states are
6 homogeneously distributed through film.
7 Guo et al reported the switching properties of *a*-$GaO_{1.2}$ thin film device are strongly
8 dependent on the electrode materials.[5] Pt is used as a top electrode material in this study
9 in order to avoid oxidation of electrode by contacting with the oxide films.
10 Resistive switching behavior of Cr-GaO_x films is strongly dependent on the
11 composition (Fig. 3). The Ga96Cr4 thin films give two orders of magnitude smaller
12 current than those of other composition and the hysteretic *I-V* curves do not appear at
13 any sweep rates (Fig. 3(a)). The others, Ga91Cr9, Ga82Cr18 and Ga78Cr22, involves
14 resistive switching at a sweep rate of 1 and 0.01 V s^{-1} (Figs. 3(b), (c) and (d)), revealing
15 a pinched hysteresis *I-V* loop in counter eight-figure clockwised polarity when the
16 voltage on TE was swept in the way of $0 \rightarrow +1 \rightarrow 0 \rightarrow -1 \rightarrow 0$ V in every composition (Fig.
17 3). A positive voltage RESET the film from the low resistance state (LRS) to the high
18 resistance state (HRS), and with negative bias the film SET to the LRS, indicating
19 bipolar resistive switching behavior of the films. Electroforming process by applying
20 high voltage is not required to initiate the switching. These results are consistent with

RSC Advances Accepted Manuscript

1 the previous studies of a-$GaO_{1.1}$ thin film devices.[5,8]

2 The hysteretic shape of *I-V* curves is strongly dependent on the voltage sweep rate,
3 see e.g. Figs. 3(b), (c) and (d). The films do not reveal hysteresis loops at fast sweep rate
4 (100 V s^{-1}), but tend to reveal wider hysteretic loops at slower rate. The switching
5 behavior is stationary and is not decayed for a few 10's voltage sweep cycles.

6 The Ga82Cr18 thin film is distinct from other composition films. The films reveal the
7 large hysteresis loop at a sweep rate of 1 and 0.01 V s^{-1} and possess the highest
8 HRS/LRS resistance ratio (on/off ratio) which is about 20 at 0.7 V (Fig. 4(a)). The ratios
9 decrease to about 2 if Cr dopant concentrations, namely, Ga(I) fractions are decreased or
10 increased as Ga91Cr9 or Ga78Cr22, respectively.

11 The area dependence of current level in Ga82Cr18 film shows linear scaling (Fig. 4b).
12 This feature discloses that the resistance state of the film below TE is homogeneously
13 changed by responding to applied field or a number of conducting filaments are
14 uniformly distributed over the electrode area.

15 In a separate experiment, we fabricated Pt/TiO_x/Pt thin film devices by the similar
16 sputtering deposition processes as reported elsewhere.[17] Rutile-type TiO_x thin films with
17 a 100 nm thickness was uniformly formed on Pt electrode, as confirmed by TEM and
18 ED patterns (Fig. S1a). The TiO_x thin film prepared here reveal the similar switching
19 behavior as the filamentary mechanism switching TiO_x devices reported previously.[2,4]
20 *I-V* hysteretic shape is not varied by decreasing the voltage sweep rate (Fig. S1b) in the

RSC Advances Accepted Manuscript

1 range of less than 100 V s^{-1}. The current level is independent on Pt TE area (Fig. 4b).
2 This is peculiar to the resistive switching triggered by variation of local states such as
3 formation and deformation of the conductive filament.

4 It is evident that resistive switching of Cr-GaO_x is quite different from TiO_x. The
5 strongly time-dependent switching events and area dependent current level is
6 incompatible with the filamentary mechanism as operating in TiO_x devices. It is
7 concluded the resistive switching of Cr-GaO_x films is driven by variation of bulk
8 states.[8,18]

9 The bulk switching mechanism suggests the film resistance can be incrementally
10 adjusted by tuning the duration and sequence of the applied bias.[19] Unlike the devices
11 with abrupt switching characteristics where the programming bias control the final
12 device state,[20,21] each programming pulse controls the relative change of the film
13 resistance in case of Cr-GaO_x devices because donor concentration profiles across film
14 can be varied sequentially by the migration at each programing bias. Figure 5 shows the
15 resistance state change of Ga82Cr18 films when a series of 70 identical negative (-0.95
16 V, 500 μs) pulses was applied on the films, followed by a series of 70 identical positive
17 voltage pulses (0.95 V, 500 μs). The large pulse bias (namely -0.95 V or 0.95 V)
18 programs the resistance state of the films and a small read bias of 0.1 V measures a
19 response current to represent the resistance state. As expected from the DC
20 characteristics of the device, the application of negative voltage pulses (-0.95 V)

RSC Advances Accepted Manuscript

incrementally decreases the film resistance, and the application of positive voltage pulses (+0.95 V) incrementally increases the resistance.

Discussion

It is clear from the results of XPS and STEM-EDX measurements (Figs. 1 and 2) that co-sputtered Cr(0) metallic atoms scavenge oxygen from adjacent Ga(III) oxide moieties by the following redox reaction

$$2Cr(0) + 3Ga(III) \rightarrow 2Cr(III) + 3Ga(I) \quad (1)$$

The chemical composition of the resultant film can be given by

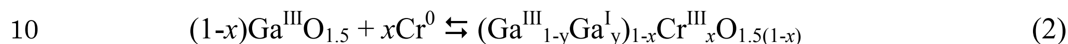

$$(1\text{-}x)Ga^{III}O_{1.5} + xCr^{0} \leftrightarrows (Ga^{III}{}_{1\text{-}y}Ga^{I}{}_{y})_{1\text{-}x}Cr^{III}{}_{x}O_{1.5(1\text{-}x)} \quad (2)$$

Then the charge balance yields:

$$y = 1.5x\ (1\text{-}x)^{-1} \quad (3)$$

The reaction (3) clarify the amount of oxygen deficiency ($1.5x$) is related to Ga(I) fraction (y). The molar fractions of Ga(I) of the films prepared here are in agreement with the values calculated by reaction (3) (Table 1). It is apparent that oxygen deficiency is involved by the reaction (2) during cosputtering.

The switching performance of Cr-GaO_x thin films is drastically changed by Ga(I) fractions (Fig. 3). The schematic model of bulk mechanism switching of gallium oxide base thin films is shown in Fig. 6. The positive bias on small area TE accumulates negatively-charged oxide ions in vicinity of TE blocking electrode by extinguishing

RSC Advances Accepted Manuscript

electron carriers so as to form highly-resistive, oxygen-rich layer near TE as follows (Fig. 6(a)).

$$Ga(I)O_{0.5} + 2e' + O \leftrightarrows Ga(III)O_{1.5} \quad (4)$$

The opposite bias can enrich the electron carriers in the layer again by driving oxide ions towards large area BE (Fig. 6(b)). At fast voltage sweep rate, the resistance ratio between HRS and LRS, namely the hysteretic width of I-V loop tends to be small because the shift of oxygen vacancy donor distribution cannot be largely changed due to the relatively short bias duration. However, the hysteresis becomes wider at slower sweep rate due to the large shift in donor distribution by longer bias duration.

Based on the mechanism, the poor resistive switching performance of low Ga(I) fraction films, such as Ga96Cr4, can be related to the poor oxide ion conductivity because the low oxygen deficiency may not afford sufficient space for the pathway of oxide ion migration. The Cr(III) contents is not beneficial for the oxide ion conduction, since the dissociation of Cr-O bonding require relatively large energy. This might be one of the reasons for the deteriorated switching performance of the high chromium content films, Ga78Cr22 (Fig. 3d). The current results suggest that the optimal molar fraction of Cr/Ga is nearly 18/82 in the relation to fast oxide ion conduction in highly oxygen deficient glass matrices.

The resistive switching performance of 120 nm-thick Ga82Cr18 thin films is superior to that of the GaO_x films (x = 1.1-1.2) given by PLD in previous studies.[5,8] The

RSC Advances Accepted Manuscript

1 former exhibits the on/off ratio of 20 at 0.7 V, however, the ratios of the later is about 2
2 at the same voltage. These results reveal the oxide glass network of the cosputtered
3 Ga82Cr18 films retain the efficient oxide ion conductivity as much as the PLD films.
4 The Ga82Cr18 film exhibits remarkable multiple resistance states as responding to short
5 pulse biasing (Fig. 5), indicating that the significant shift of oxygen vacancy donors for
6 resistance change can be induced by the bias duration of 100's μs.

7 The oxide ion mobility in M-doped GaO_x thin films may be largely varied by choice
8 of dopant cations as is the case with various ceramic oxide ion conductors.[22] Except for
9 chromium, various metals such as Mg, Ti, Al etc. are potential candidates as oxygen
10 scavenging dopant of Ga_2O_3 from the view point of M-O bond formation energy.
11 Recently, Chang et al reported oxygen-deficient, amorphous WO_x thin film also shows
12 multiple resistive switching probably due to oxide ion conduction.[23] This suggests that
13 not only the gallium oxide but also other nonstoichiometric metal oxide systems can be
14 considered as a possible candidate of bulk oxide ion conducting thin films. Most of
15 metals and binary metal oxides can be used as a target material of rf sputtering
16 techniques. It is concluded that the cosputtering with a pair of resistive switching oxides
17 and oxygen scavenging metal dopant affords a strong tool to tune the oxide ion
18 conductivity of the highly-nonstoichiometric, resistive switching metal oxide thin films.
19

20 **Conclusion**

RSC Advances Accepted Manuscript

1 In summary, the fabrication method of Cr-doped gallium oxide thin films with
2 tailored gallium valence state and oxygen deficiencies has been established, based on
3 the reactive cosputtering with Ga_2O_3 and Cr targets. The Ga(I)-Ga(III) mixed valence
4 state homogeneous oxide glass can be formed from a homogeneous mixture of Cr(0)
5 metal atoms and Ga(III) oxides moieties deposited by cosputtering, because Cr(0)
6 scavenges oxygen of Ga(III) oxide due to the relatively large negative energy of Cr-O
7 bonding in comparison to Ga-O bonding. The Ga82Cr18 thin film with optimal Ga(I)
8 contents can reveal remarkable homogeneous resistance switching due to the efficient
9 bulk oxide ion conduction. The on/off ratio of the film is similar to that of the
10 highly-nonstoichiometric $GaO_{1.1}$ thin films prepared by PLD. The film clearly involves
11 multiple resistance state switching where the final device state is determined by bias
12 history, since the oxygen vacancy donor profiles can be incrementally modified by bias
13 duration or number of the applied short pulse biasing. The current results open up a new
14 way to design the bulk mechanism resistive switching metal oxide thin films with
15 tailored oxide ion conductivity.
16
17 **Acknowledgement**

18 This work was conducted at Hokkaido University, supported by "Nanotechnology
19 Platform" program of the MEXT Japan. CK was supported by the MEXT Japan through
20 program for Leading Graduate Schools (Hokkaido University "Ambitious Leader's

RSC Advances Accepted Manuscript

1 Program"). YA is grateful for financial support for his stay in RWTH-Aachen by the
2 Deutsche Forschungsgemeinschaft (DFG) within the SFB 917 "Nanoswitches".
3

4 **Reference**

5 1. D. B. Strukov, G. S. Snider, D. R. Stewart and R. S. Williams, *Nature*. 2008, **453**,
6 80; R. Waser, R. Dittmann, G. Staikov and K. Szot, *Adv. Mater.*, 2009, **21**, 2632.
7 2. J. J. Yang, M. D. Pickett, X. Li, D. A. A. Ohlberg, D. R. Stewart and R. S. Williams,
8 *Naure Nanotechnol.*, 2008, **3**, 429; K. K. Min, J. D. Seok and H. C. Seong,
9 *Nanotechnol.*, 2011, **22**, 254002; D.-H. Kwon, K. M. Kim, J. H. Jang, J. M. Jeon, M.
10 H. Lee, G. H. Kim, X.-S. Li, G.-S. Park, B. Lee, S. Han, M. Kim and C. S. Hwang,
11 *Nature Nanotechnol.*, 2010, **5**, 148; Y. Sato, K. Kinoshita, M. Aoki, and Y.
12 Sugiyama, *Appl. Phys. Lett.*, 2007, **90**, 033503. J. P. Strachen, M. D. Pickett, J. J.
13 Yang, S. Aloni, A. L. D. Kilcoyne, G. M. Ribeiro and R. S. Williams, *Adv. Mater.*,
14 2010, **22**, 3573; J. H. Hur, M.-J. Lee, C. B. Lee, Y.-B. Kim and C.-J. Kim, *Phys. Rev.*
15 *B.*, 2010, **82**, 155321.
16 3. R. Muenstermann, T. Menke, R. Dittmann, and R. Waser, *Adv. Mater.*, 2010, **22**,
17 4819.
18 4. M. D. Pickett, D. B. Strukov, J. L. Borghetti, J. J. Yang, G. S. Snider, D. R. Stewart
19 and R.S. Williams, *J. Appl. Phys.*, 2011, **106**, 074508; F. Alibert, L. Gao, B. D.
20 Hoskins and D. B. Strulov, *Nanotechnol.*, 2012, **23**, 075201.

RSC Advances Accepted Manuscript

1 5. X. Gao, Y. Xia, J. Ji, H. Xu, Y. Su, H. Li, C. Yang, H. Guo, J. Yin and Z. Liu, *Appl.*
2 *Phys. Lett.*, 2010, **97**, 193501.
3 6. D.-Y. Lee and T.-Y. Tseng, *J. Appl. Phys.*, 2010, **110**, 114117
4 7. D. Y. Guo, Z. P. Wu, Y. H. An, P. G. Li, P. C. Wang, X. L. Chu, X. C. Guo, Y. S. Zhi,
5 M. Lei, L. H. Li and W. H. Tang, *Appl. Phys. Lett.*, 2015, **106**, 042105; X. B. Yan,
6 H. Hao, Y. F. Chen, Y. C. Li and W. Banerjee, *Appl. Phys. Lett.*, 2014, **105**, 093502;
7 D. Y. Guo, Z. P. Wu, L. J. Zhang, T. Yang, Q. R. Hu, M. Lei, P. G. Li, L. H. Li and
8 W. H. Tang, *Appl. Phys. Lett.*, 2015, **107**, 032104; J. B. Yang, T. C. Chang, J. J.
9 Huang, S. C. Chen, P. C. Yang, Y. T. Chen, H. C. Tseng, S. M. Sze, A. K. Chu and
10 M. J. Tsai, *Thin Solid Films*, 2013, **529**, 200; C. W. Hsu and L. J. Chou, *Nano Lett.*,
11 2012, **12**, 4247.
12 8. Y. Aoki, C. Wiemann, C. Fayer, H.-S. Kim, C.M. Schneider, H. I. Yoo and M.
13 Martin, *Nature Commun.*, 2014, **5**, 4473.
14 9. L. Nagarajan, R. A. DeSouza, D. Samuelis, I. Valov, A. Borger, J. Janek, K.-D.
15 Becker, P. C. Schmidt and M. Martin, *Nature Mater.*, 2008, **7**, 391.
16 10. J. J. Yang, D. B. Strukov and D. R. Stewart, *Nature Nanotechnol.*, 2013, **8**, 13.
17 11. T. Chang, S. H. Jo, H. K. Kim, P. Sheridan, S. Gaba and W. Lu, *Appl. Phys. A*, 2011,
18 **102**, 857.
19 12. D. G. Kolman, T. N. Taylor, Y. S. Park, M. Stan, D. P. Butt, C. J. Maggiore, J. R.
20 Tesmer and G. J. Havrille, *Oxidat. Metal*, 2001, **56**, 347.

RSC Advances Accepted Manuscript

1 13. D. R. Lide, *Handbook of Chemistry and Physics, 84th ed.*, CRC Press, 2003, 74.
2 14. R. Carli and C. L. Bianchi, *Appl. Surf. Sci.*, 1994, **74**, 99; C. C. Surdu-Bob, S. O.
3 Saied and J. L. Sullivan, *Appl. Surf. Sci.*, 2001, **183**, 126.
4 15. K. Petkov, V. Krastev and T. Marinova, *Surf. Interf. Anal.*, 1992, **18**, 487.
5 16. J. Sainio, M. Aronniem, O. Pakarinen, K. Kauraal, S. Airaksine, O. Krause and J.
6 Lahtinen, *Appl. Surf. Sci.*, 2005, **252**, 1076.
7 17. D. S. Jeong, H. Schroeder and R. Waser, *Appl. Phys. Lett.*, 2006, **89**, 082909; D. S.
8 Jeong, H. Schroeder and R. Waser, *Electrochem. Solid State Lett.*, 2007, **10**, G51.
9 18. R. Meyer, L. Schloss, J. Brewer, R. Lambertson, W. Kinney. J. Sanchez and D.
10 Rimerson, *IEEE Proceed. NVMTS2008*, 2008, 1.
11 19. Y. B. Nian, J. Strozier, N. J. Wu, X. Chen and A. Ignatiev, *Phys. Rev. Lett.*, 2007,
12 **98**, 146403.
13 20. M. J. Lee, S. Han, S. H. Jeon, B. H. Park, B. S. Kang, S. E. Ahn, K. H. Kim, C. B.
14 Lee, C. J. Kim, I. K. Yoo, D. H. Seo, X. S. Li, J. B. Park, J. H. Lee and Y. Park,
15 *Nano Lett.*, 2009, **9**, 1476.
16 21. S. H. Jo, K. H. Kim and W. Lu, *Nano Lett.*, 2009, **9**, 496.
17 22. S. Grieshammer, B. O. H. Grope, J. Koettgen and M. Martin, *Phys. Chem. Chem.*
18 *Phys.*, 2014, **16**, 9974; S. G. Kang and D. S. Sholl, *RSC. Adv.*, 2013, **3**, 3333.
19 23. T. Chang, S. H. Jo and W. Lu, *ACS Nano*, 2011, **5**, 7669; S. H. Jo, T. Chang, I.
20 Ebong, B. B. Bhadviya, P. Muzumder and W. Lu, *Nano Lett.*, 2010, **10**, 1297.

RSC Advances Accepted Manuscript

1

2 Table 1 List of the sputtering power of Cr for Cr-Ga_2O_3 cosputtering deposition and

3 composition and Ga(III) /Ga(I) molar ratios of the corresponding Cr-GaO_x thin films.

4

Rf power / W	Name	Composition #	Ga(III) / Ga(I) ϒ	Ga(III) / Ga(I) ∀
70W	Ga78Cr22	$Ga_{0.78\pm0.06}Cr_{0.22\pm0.03}O_{1.2\pm0.1}$	61/39	58/42
60 W	Ga82Cr18	$Ga_{0.82\pm0.2}Cr_{0.18\pm0.02}O_{1.2\pm0.1}$	69/31	67/33
40 W	Ga91Cr9	$Ga_{0.91\pm0.04}Cr_{0.09\pm0.05}O_{1.3\pm0.1}$	77/23	85/15
30 W	Ga96Cr4	$Ga_{0.96\pm0.02}Cr_{0.04\pm0.02}O_{1.4\pm0.1}$	90/10	93/7

5 # determined by WDX. ϒ determined by XPS. ∀ calculated by eq (3).

6

7

RSC Advances Accepted Manuscript

1 **Figure captions**

2

3 Fig. 1 (a) Cross-section TEM image and (b) ED pattern of Ga82Cr12 thin films.
4 Corresponding elemental EDX mapping of (c) Ga and (d) Cr.

5

6 Fig. 2 Fig. 2 (a) Ga 3d and (b) Cr 2*p* XPS spectra of 120 nm-thick thin films of (a1&b1)
7 Ga78Cr22, (a2&b2) Ga82Cr18, (a3&b3) Ga91Cr9 and (a4&b4) Ga96Cr4. (c) Ga 3*d*
8 XPS depth profile of 120 nm-thick Ga82Cr18 thin films. The spectra were stored at the
9 surface (c1) and at the points in 60 nm (c2) and 100 nm depth (c3). Red dots are the
10 observed and black lines the simulated.

11

12 Fig. 3 *I-V* characteristics of Pt(TE)/Cr-GaO_x film/Pt(BE) devices thickness during a
13 repeated voltage sweep cycle of 0 → +1 → -1 → 0 V at different voltage sweep rates.
14 (a1)-(a3) Ga92Cr4, (b1)-(b3) Ga91Cr9, (c1)-(c3) Ga82Cr18 and (d1)-(d3) Ga78Cr22
15 thin films with 120 nm thickness. The sweep rate is 100 V s^{-1} in (a1), (b1), (c1) and (d1),
16 1 V s^{-1} in (a2), (b2), (c2) and (d2) and 0.01 V s^{-1} in (a3), (b3), (c3) and (d3). The cycles
17 are repeated 20 time in (c2) and 10 time in others. The numbered arrows indicate the
18 direction of the switching cycles (counter-figure-eight loops). 1st, 10th and 20th curves
19 are shown by blue, red and green, respectively. The curves of other cycles are shown by
20 black. The current levels in (a1)-(a3) are multiplied by 30.

RSC Advances Accepted Manuscript

1

2 Fig. 4 (a) On/Off switching ratio vs Cr content at 0.7 V, measured at a voltage sweep
3 rate of 100(+), 1(○) and 0.01(△) V s^{-1}. (b) TE area scaling of the current of LRS
4 Ga82Cr18 and TiO_x thin films at -0.5 V.

5

6 Fig. 5 Current response transients of Ga82Cr18 thin films, measured by applying 500 μs
7 programming bias (+0.95 or -0.95 V) and 100 μs read bias (+0.1 V). Red is the current
8 measured at 0.1 V read pulse after programmed by a -0.95 V pulse and blue is the one
9 after programmed by a 0.95 V pulse. The insets show pulse patterns used for the
10 measurements.

11

12 Fig. 6 Schematic representation of bulk mechanism resistive switching in Cr-GaO_x thin
13 film devices. (a) Positive bias and (b) negative bias on TE.

14

15

16

RSC Advances Accepted Manuscript

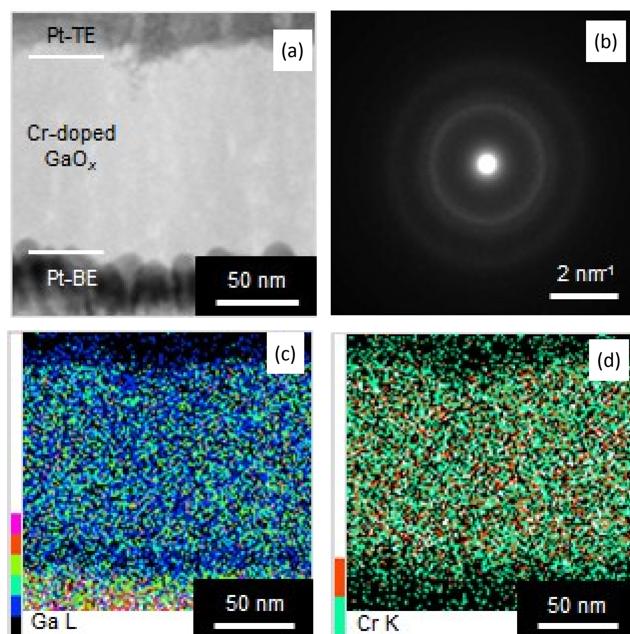

Fig. 1 (a) Cross-section TEM image and (b) ED pattern of Ga82Cr18 thin films. Corresponding elemental EDX mapping of (c) Ga and (d) Cr.

RSC Advances Accepted Manuscript

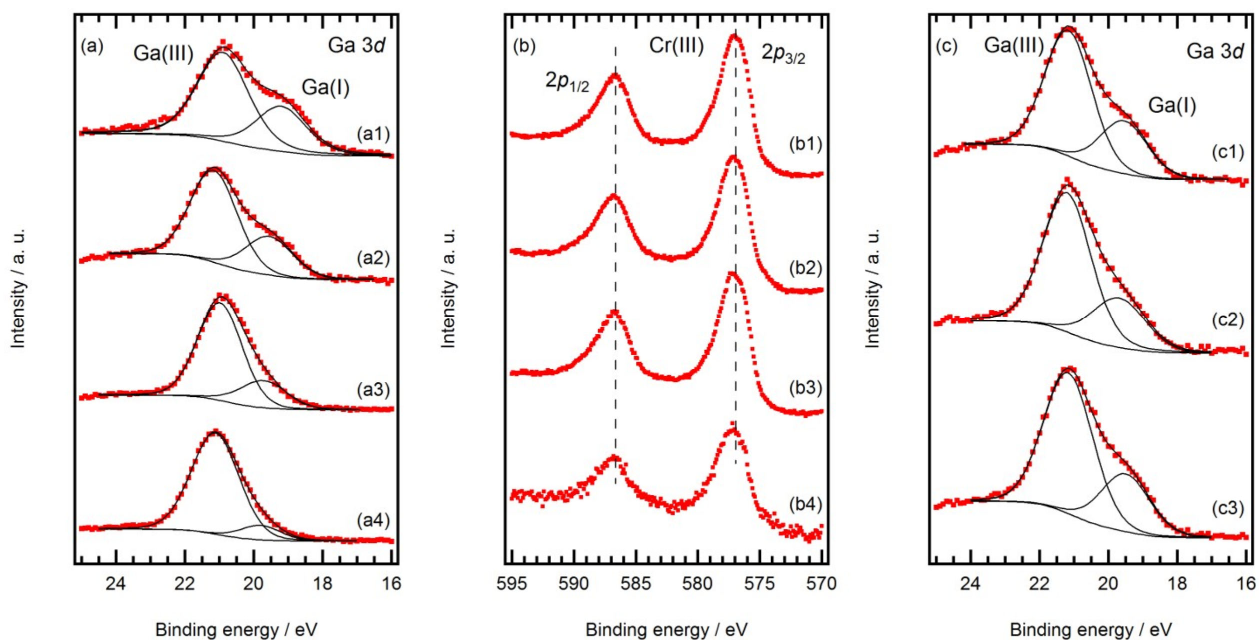

Fig. 2 (a) Ga 3d and (b) Cr 2*p* XPS spectra of 120 nm-thick thin films of (a1&b1) Ga78Cr22, (a2&b2) Ga82Cr18, (a3&b3) Ga91Cr9 and (a4&b4) Ga96Cr4. (c) Ga 3*d* XPS depth profile of 120 nm-thick Ga82Cr18 thin films. The spectra were stored at the surface (c1) and at the points in 60 nm (c2) and 100 nm depth (c3). Red dots are the observed and black lines the simulated.

RSC Advances Accepted Manuscript

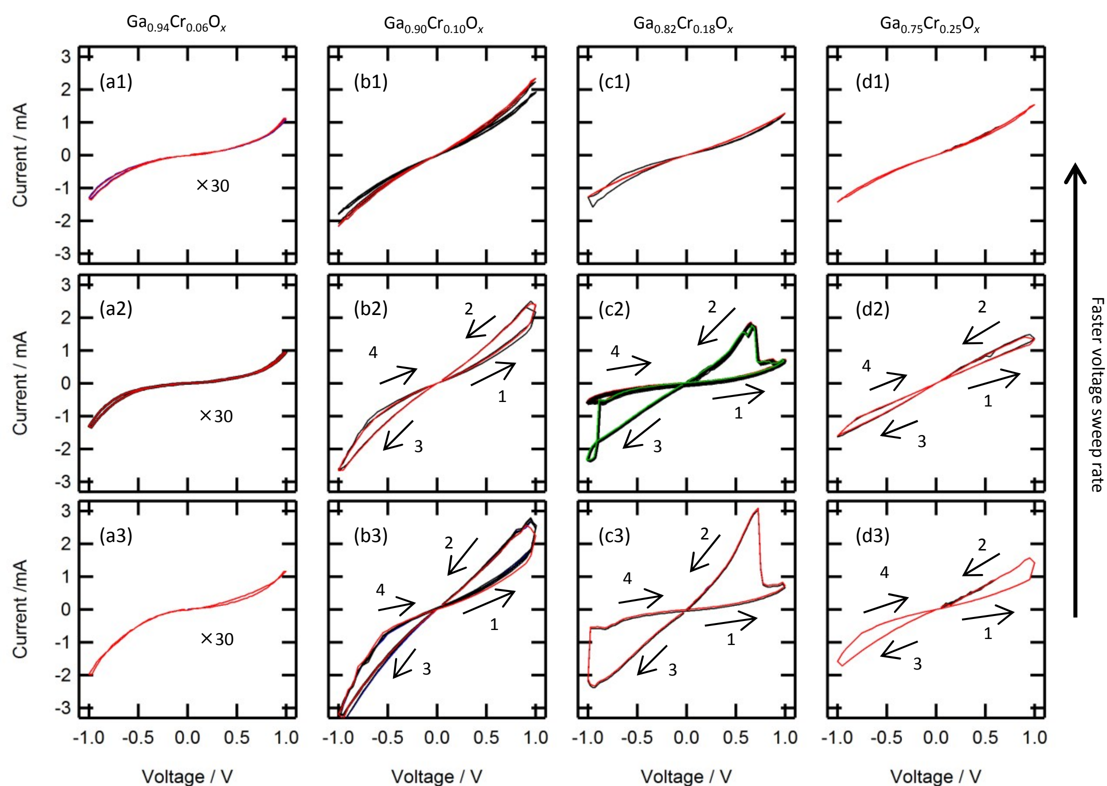

Fig. 3 *I-V* characteristics of Pt(TE)/Cr-GaO_x film/Pt(BE) devices thickness during a repeated voltage sweep cycle of 0 $\rightarrow$ +1 $\rightarrow$ -1 $\rightarrow$ 0 V at different voltage sweep rates. (a1)-(a3) Ga92Cr4, (b1)-(b3) Ga91Cr9, (c1)-(c3) Ga82Cr18 and (d1)-(d3) Ga78Cr22 thin films with 120 nm thickness. The sweep rate is 100 V s^{-1} in (a1), (b1), (c1) and (d1), 1 V s^{-1} in (a2), (b2), (c2) and (d2) and 0.01 V s^{-1} in (a3), (b3), (c3) and (d3). The cycles are repeated 20 time in (c2) and 10 time in others. The numbered arrows indicate the direction of the switching cycles (counter-figure-eight loops). 1st, 10th and 20th curves are shown by blue, red and green, respectively. The curves of other cycles are shown by black. The current levels in (a1)-(a3) are multiplied by 30.

RSC Advances Accepted Manuscript

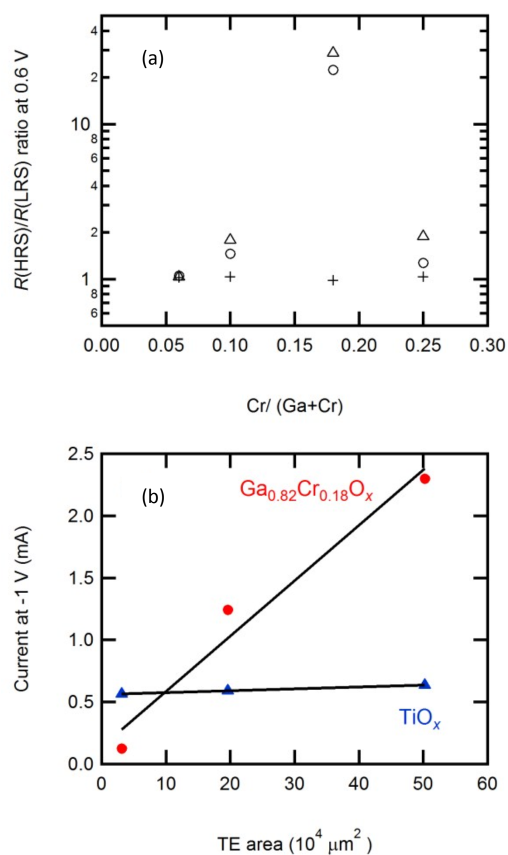

Fig. 4 (a) On/Off switching ratio vs Cr content at 0.7 V, measured at a voltage sweep rate of 100(+), 1(○) and 0.01(△) V s^{-1}. (b) TE area scaling of the current of LRS Ga82Cr18 and TiO_x thin films at -0.5 V.

RSC Advances Accepted Manuscript

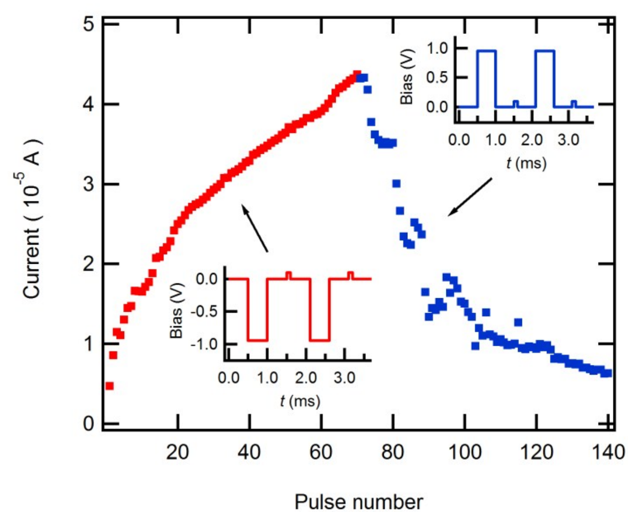

Fig. 5 Current response transients of Ga82Cr18 thin films, measured by applying 500 μs programming bias (+0.95 or -0.95 V) and 100 μs read bias (+0.1 V). Red is the current measured at 0.1 V read pulse after programmed by a -0.95 V pulse and blue is the one after programmed by a 0.95 V pulse. The insets show pulse patterns used for the measurements.

RSC Advances Accepted Manuscript

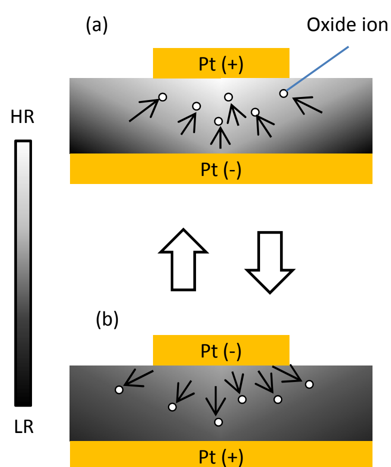

Fig. 6 Schematic representation of bulk mechanism resistive switching in Cr-GaO_x thin film devices. (a) Positive bias and (b) negative bias on TE.

RSC Advances Accepted Manuscript

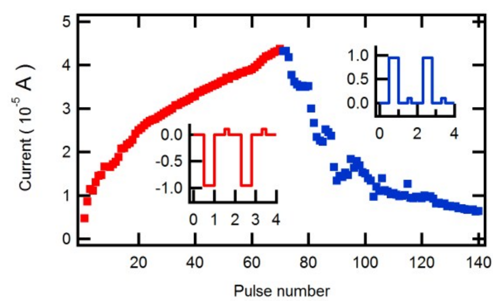

Cr-GaO_x film resistance can be incrementally adjusted by tuning the duration and sequence of the applied bias.

RSC Advances Accepted Manuscript